

BeppoSAX detection of the Fe K line in the nearby starburst galaxy NGC 253

M. Persic¹, S. Mariani², M. Cappi³, L. Bassani³, L. Danese⁴, A.J. Dean⁵, G. Di Cocco³, A. Franceschini⁶, L.K. Hunt⁷, F. Matteucci⁸, E. Palazzi³, G.G.C. Palumbo^{2,3}, Y. Rephaeli⁹, P. Salucci⁴, and A. Spizzichino³

¹ Trieste Astronomical Observatory, via G.B. Tiepolo 11, 34131 Trieste, Italy

² Astronomy Dept., University of Bologna, via Zamboni 33, 40126 Bologna, Italy

³ ITeSRE/CNR, via Gobetti 101, 40129 Bologna, Italy

⁴ SISSA/ISAS, via Beirut 2-4, 34013 Trieste, Italy

⁵ Physics Dept., Southampton University, Southampton SO9 5NH, UK

⁶ Astronomy Dept., University of Padova, vicolo dell'Osservatorio 5, 35122 Padova, Italy

⁷ CAISMI/CNR, Largo E. Fermi 5, 50125 Firenze, Italy

⁸ Astronomy Dept., University of Trieste, via Besenghi, 34131 Trieste, Italy

⁹ School of Physics and Astronomy, Tel Aviv University, Tel Aviv 69978, Israel

Received.....; accepted.....

Abstract. We present *BeppoSAX* results on the nearby starburst galaxy NGC 253. Although extended, a large fraction of the X-ray emission comes from the nuclear region. Preliminary analysis of the LECS/MECS/PDS ~ 0.2 –60 keV data from the central $4'$ region indicates that the continuum is well fitted by two thermal models: a “soft” component with $kT \sim 0.9$ keV, and a “hard” component with $kT \sim 6$ keV absorbed by a column density of $\sim 1.2 \times 10^{22} \text{ cm}^{-2}$. For the first time in this object, the Fe K line at 6.7 keV is detected, with an equivalent width of ~ 300 eV. This detection, together with the shape of the 2–60 keV continuum, implies that most of the hard X-ray emission is thermal in origin, and constrains the iron abundances of this component to be ~ 0.25 of solar. Other lines clearly detected are Si, S and Fe L/Ne, in agreement with previous *ASCA* results. We discuss our results in the context of the starburst-driven galactic superwind model.

average. In the early evolution of galaxies ($z \gtrsim 1$), star formation was certainly much higher than at present (see e.g. Madau et al. 1996; Hogg et al. 1998): a starburst phase was, therefore, normal in the early evolution of galaxies. Part of the interest in local SBGs stems then from the possibility that they resemble normal galaxies when they were at $z \gtrsim 1$. High-energy phenomena highlight the SB activity (Bookbinder et al. 1980): because of obscuration of the optical emission (by star-heated IS dust), X-rays allow a penetrating view of SBGs.

Aiming at studying the X-ray properties of local SBGs, we have undertaken a program to study two such sources, NGC 253 and M82, with *BeppoSAX*: in this Letter the broad-band spectrum of the nuclear region of NGC 253 is reported, focusing on the discovery of the Fe K line at 6.7 keV and on the features of the continuum in the 2–10 keV band arising from the nuclear region.

Assumed to be a prototypical SBG, NGC 253 has been extensively observed in X-rays. At low energies, analysis of Einstein IPC data led Fabbiano (1988) to conclude that the nuclear emission was softer and more absorbed than that from the entire galaxy. A subsequent observation by *Ginga* in the 2–10 keV band (Ohashi et al. 1990) indicated that the spectrum was best fitted by a 6–7 keV thermal bremsstrahlung and no significant absorption; no iron line emission was detected ($EW < 400$ eV). A more recent *ASCA* measurement (Ptak et al. 1997) required a two-component model to explain the complexity of the NGC 253 X-ray spectrum [i.e., a soft thermal component with $kT \sim 0.8$ keV, plus a hard absorbed ($N_H \sim 10^{22} \text{ cm}^{-2}$) component, described either as thermal ($kT \sim 7$ keV) or

Key words: Galaxies: individual: NGC 253 – Galaxies: spiral – Galaxies: starburst

1. Introduction

In the local universe, starburst galaxies (SBGs) are galaxies with current (for typically 10^8 yr: Rieke et al. 1980) star formation rates significantly higher than the galactic

Send offprint requests to: Massimo Persic;
e-mail:persic@oat.ts.astro.it

power-law ($\Gamma \sim 2$): again, no iron line emission was detected ($EW < 180$ eV). At higher energies, a 4.4σ detection by *OSSE* has been claimed by Bhattacharya et al. 1994 with a 50–165 keV flux of 3×10^{-11} ergs cm $^{-2}$ s $^{-1}$, higher than that extrapolated from the *Ginga/ASCA* observation.

2. The *BeppoSAX* observation

NGC 253 was observed on Nov.29–Dec.2, 1996 (see Table 1). The source is clearly extended (and elongated) up to $\sim 10'$ in the *BeppoSAX* image in both the 0.1–2 keV and 2–10 keV band. Analysis of the resolved emission is deferred to a separate paper (but see preliminary results in Cappi et al. 1998): here we only present the analysis of the unresolved nuclear emission. In the central $4'$ region (typical extraction region for point sources used for the LECS and MECS instruments), we obtained a LECS count rate of 3.93×10^{-2} cts s $^{-1}$ and a MECS count rate of 9.23×10^{-2} cts s $^{-1}$. Background spectra, extracted from the standard blank-sky files provided by the *BeppoSAX* Science Data Center (SDC), contributed less than about 5% and 15% at 2 and 6 keV, respectively: similar results were also obtained using background spectra extracted directly from the instruments' fields of view. LECS data above 4 keV were excluded because of remaining calibration uncertainties. LECS and MECS data were reduced using the SAXDAS v.1.3.0 and XANADU packages, while the XAS v.2.0 package was used for the PDS data. LECS and MECS spectra were rebinned in order to obtain at least 20 counts per energy channel, to allow use of the χ^2 statistics.

Table 1: Exposure times.

Instrument	En. range	Obs. time
	keV	sec
LECS	0.1-4	54689
MECS	1.3-10	113403
PDS	13-60	51557

No short or long term variability is detected from the present data in any energy band: a fact that can be simply interpreted as evidence for the large size of the emitting region. The 0.5–2 keV and 2.0–10 keV fluxes observed by *BeppoSAX* are $\sim 2.53 \times 10^{-12}$ erg s $^{-1}$ cm $^{-2}$ and 4.9×10^{-12} erg s $^{-1}$ cm $^{-2}$. These are roughly consistent with the observed ROSAT PSPC and *ASCA* fluxes (Serlemitsos et al. 1996; Ptak et al. 1997) if one takes into account the different sizes of the source regions. The global, absorption-corrected, 0.5–2 keV plus 2.0–10 keV luminosities are 7.72×10^{39} ergs s $^{-1}$ and 1.57×10^{40} ergs s $^{-1}$ for the soft and the hard component (see Table 3), respectively, for an assumed distance of 3 Mpc.

The *BeppoSAX* PDS count-rate between 13–60 keV is 0.07 ± 0.02 cts s $^{-1}$ which corresponds to a $\sim 2.5 \sigma$ level detection if systematics errors ($\sim 10\%$) are taken into account: thus the 3σ upper-limit to the PDS 50–165 keV flux is 7.1×10^{-12} ergs cm $^{-2}$ s $^{-1}$, much lower than the flux claimed to have been detected by OSSE.

In the following, $N_{\text{Hgal}} = 1.28 \times 10^{20}$ cm $^{-2}$ (Dickey & Lockman 1990) is assumed.

Table 2: Bremsstrahlung plus emission lines model.

Element ID for K $_{\alpha}$ line	Obs. Energy keV	EW eV
Fe L, Ne IX/X	$0.95^{+0.03}_{-0.04}$	109^{+44}_{-42}
Si XIV/XV	$1.91^{+0.04}_{-0.04}$	67^{+23}_{-23}
S XV	$2.42^{+0.04}_{-0.06}$	79^{+34}_{-34}
Fe XXV	$6.69^{+0.07}_{-0.07}$	329^{+89}_{-109}

Notes: The value of the relative normalizations $A_{\text{LECS}}/A_{\text{MECS}}$ is $0.64^{+0.04}_{-0.03}$. Intervals are at 90% confidence for one interesting parameter.

* Line energy fixed to the *ASCA* value (Ptak et al. 1997).

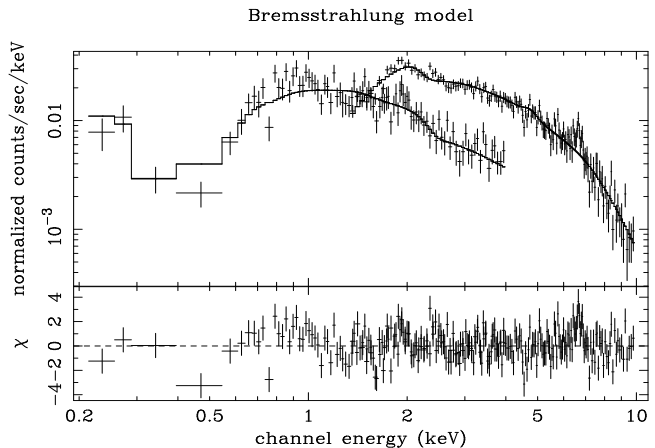


Fig. 1. Thermal bremsstrahlung fit to the MECS and LECS data; the lines stand out clearly on the continuum.

3. Spectral analysis

We first used a thermal bremsstrahlung continuum plus emission lines model to parameterize the line energies and intensities. The LECS and MECS spectra were fitted simultaneously, with free relative normalization. The best-

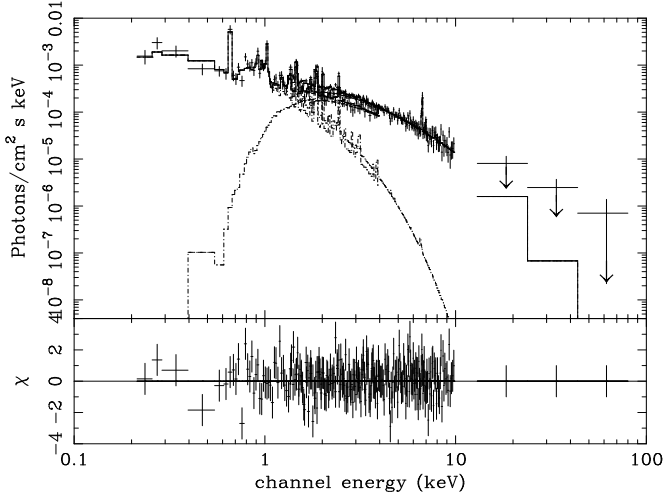


Fig. 2. Variable-abundances Mekal model fit to the MECS, LECS and PDS data.

fit value for the central temperature is $kT = 7.40^{+0.18}_{-0.71}$ (with $\chi^2/\text{dof}=254/232$). A few emission lines are evident in Fig.1: their resulting intensities and energies are listed in Table 2. In agreement with the *ASCA* results, most lines are consistent with K_α emission from H-like and He-like ions.

At low energies ($E \lesssim 3$ keV) the strong emission lines, notably the residual broad excess at $E < 1$ keV (a clear signature of the Fe L/Ne complex), require: (a) a soft thermal component with $kT < 1$ keV; and (b) that the hard component be absorbed in order not to overproduce the continuum for $E \lesssim 0.7$ keV (see also Ptak et al. 1997).

At higher energies, an Fe K line at ~ 6.7 keV is unambiguously detected for the first time in NGC 253. It is narrow ($\sigma < 0.13$ keV), with $EW = 330$ eV and consistent with emission from Fe XXV. [The measured equivalent width is roughly consistent with the upper limits placed by previous studies (Ohashi et al. 1990; Ptak et al. 1997) if one considers that those authors used a flatter power-law continuum.] Moreover, compared with *ASCA*, the larger MECS effective area at $E > 7$ keV allows us to firmly establish that the 2–10 keV continuum is dominated by thermal emission, since a hard power law alone (still allowed by the *ASCA* data: Ptak et al. 1997) yields a significantly worse fit ($\Delta\chi^2=20$) with the present data.

A two-temperature plasma is also required by the following consideration. An atomic line energy is a function of the electron temperature kT and the degree of ionization (measured by $n_e t$, where n_e is the electron density and t the elapsed time). The centroids of the identified K-lines (Fe, Mg, Si, S: see Table 2), imply allowable kT - $n_e t$ regions (see Fig.2b of Kaneda et al. 1997) that are not compatible with a single-temperature plasma. Thus, at least two plasma components (with different ionization states) are required in order to reproduce the observed SAX spectrum of NGC 253.

Therefore our best-fit model consists of a two-component thermal model. Best-fit parameters are reported in Table 3 for a two-temperature Raymond-Smith model and a two-temperature Mewe-Kaastra-Liedah plasma model (“mekal” in XSPEC). In order to reduce the number of free parameters, the abundances of He, C, and N were fixed at the solar value. The heavier elements were divided into two groups: Fe and Ni (most likely associated with SNe I products), and the α -elements O, Ne, Mg, Si, S, Ar and Ca (most likely associated to SNe II products); elements in the same group were constrained to have common abundances in solar units.

Both components have consistent features within the statistical errors. The detection of the Fe K line in NGC 253 allows us to reliably determine the Fe abundance in the line-emitting gas in the hard component: we find a value of ~ 0.25 solar, again consistent with the sub-solar values (based on upper limits) predicted by Ohashi et al. (1990) and Ptak et al. (1997). The iron abundance of the soft component is also constrained to a similar value. Instead, the abundances of the α -elements are consistent with a single value of ~ 1.7 solar, for both spectral components.

4. Discussion and Conclusions

The likely emission mechanisms and environments for X-ray emission in SBGs have been described by Rephaeli et al. (1995). In general, they may include thermal emission from SNe, SNRs, and hot gas in the disk and halo, and nonthermal emission from massive X-ray binaries and Compton scattering of relativistic electrons off the FIR and CMB fields in the disk and the halo. Combined with the extent of the source of the 2–10 keV emission, the detection of the spectral lines reported here is a strong evidence for thermal hard X-ray emission from hot gas in SNRs and/or SN-driven wind, and severely limits any contribution from a nuclear low-luminosity AGN.

A remarkable result from the present analysis is the striking similarity between the *BeppoSAX* spectrum of NGC 253 and the *ASCA* 0.6–10 keV spectrum of the Galactic Ridge X-Ray Emission (GRXE) in the Scutum arm region (Kaneda et al. 1997), i.e. unresolved diffuse X-ray emission components distributed in a thin disk along the Milky Way. The derived temperatures of both thermal continua and the identified lines with their centroid energies are similar for NGC 253 and the GRXE.

Following Kaneda et al.’s detailed analysis of the GRXE soft component, the departure from ionization equilibrium that can be similarly inferred in the soft component of NGC 253 suggests that such component may be due to SNR-related emission from a diffuse plasma. For an estimated SNR luminosity of $\sim 2 \times 10^{35}$ erg s $^{-1}$ (see Kaneda et al. 1997), it can be estimated that the soft component’s 0.5–10 keV luminosity is powered by $\sim 4 \times 10^4$ SNRs. The lack of appreciable photoelectric absorption,

implying a low HI column density where the soft component originates, also supports this galactic superwind picture. The derived chemical abundances of the soft component (see Table 2), that agree with the predictions of superwind and SBG chemical evolution models (Suchkov et al. 1994; Bradamante et al. 1998), favour too the galactic wind picture. In such models the galactic wind is powered mostly by Type II SNe and minimally by Type Ia SNe: since Type II SNe eject mostly α -elements and Type Ia SNe eject mostly Fe, the resulting wind is overabundant in α -elements and underabundant in Fe. It should be noted, however, that uncertainties in the absorbing HI column density and the likely spread of plasma temperatures may substantially affect the derived chemical abundances (see Read et al. 1997; Dahlem et al. 1998).

The origin of the extended, thermal hard component is less clear. The substantial photoelectric absorption obtained from our best-fit requires a high in-situ hydrogen column density, $N_H \sim 1.3 \times 10^{22} \text{ cm}^{-2}$ (also the nuclear radio emission suggests the presence of molecular gas with similar column density: Nakai et al. 1987; Paglione et al. 1996). This suggests that the hard component may originate in buried, actively star-forming regions, with Type II SNe and X-ray binaries possibly supplying the bulk of the X-ray emission and the ambient gas and dust providing the intrinsic absorption. In any case, this thermal plasma cannot be in equilibrium as it is not confined by galactic gravity. To estimate the contribution of SNe to the observed thermal flux, assuming that Type II SNe dominate the heating of the ISM, we repeat the swept-up mass calculation of Ptak et al. (1997) and similarly obtain that $\lesssim 50\%$ of the hard component originates in superwind emission and not in the ambient ISM. The chemical abundances of the hard component, consistent with those deduced for the soft component, are likewise in agreement with the trend expected for SB-driven superwind models and hence are compatible with the SN origin for (a substantial fraction of) the hard component. Moreover, Fe could be further depleted (relative to S and Si) by NGC 253's plentiful dust and warm ISM clouds (see Telesco 1988).

However, the galactic wind interpretation of NGC 253's hard component raises some basic questions: (i) what is the mechanism leading to the high $\sim 6 \text{ keV}$ temperature?, and (ii) how many SNRs are required to power the hard emission? In fact: (1) SNRs usually have substantially lower temperatures ($kT \lesssim 4 \text{ keV}$); (2) even neglecting the spectral discrepancy, if $L_X^{\text{SNR}} \sim 2 \times 10^{35} \text{ erg s}^{-1}$ then $\gtrsim 8 \times 10^4$ SNRs are required to power the hard component of NGC 253, while $n_{\text{SNR}} < 7.5 \times 10^4 \left(\frac{R_{\text{SB}}}{5 \text{ kpc}}\right)^2 \left(\frac{z_{\text{SB}}}{0.5 \text{ kpc}}\right) / \frac{4}{3} \left(\frac{R_{\text{SNR}}}{0.05 \text{ kpc}}\right)^3$ (where R_{SB} and z_{SB} are the radius and thickness of the SB region, and R_{SNR} is the SN shock front) SNRs can be at work if the two-phase status of NGC 253's ISM is to be preserved. Alternatively, the estimated $\sim 4 \times 10^4$ SNRs powering the soft component contribute only $< 50\%$ of the hard component; and

(3) hydrodynamical simulations of superwinds do predict hard X-ray emission at such high temperatures, but with lower luminosities (compared to the soft X-ray component) and higher metal abundances (Suchkov et al. 1994): however, a self-consistent model of galaxy formation and evolution, including baryon infall and dissipation, star formation, and feed-back onto the still infalling gas, is required to test the superwind picture (eg., Heckman et al. 1990) in detail.

Alternative explanations of the hard component involve either (1) a different mechanism leading to the observed thermal emission or (2) a "spectral conspiracy" (discussed in a separate paper) between a softer thermal emission and non-thermal emission yielding the observed spectrum. As for the former case, a magnetic confinement picture (e.g., Makishima 1994, 1995) entails that some fraction of the cooler plasma, confined by magnetic loops in the galactic disk, is heated to the observed temperature by the dissipation of the galaxy's rotational and velocity-dispersion energy through magnetic compression and reconnection. As for non-thermal spectral components, the two most likely candidates are X-ray binaries and Compton scattering of nuclear IR flux by relativistic electrons (Rephaeli et al. 1995; other nonthermal processes are discussed by Valinia & Marshall 1998). As concerns point-like sources, Ptak et al. (1997), fitting *ASCA* SIS spectra for two strong extranuclear point sources by a Raymond-Smith plus power-law model, argue that the sources' fit parameters are similar to those for the entire galaxy, and the two points make up $\sim 25\%$ of the $2 - 10 \text{ keV}$ flux. While some of the point sources in NGC 253 are associated with SNe, some others are likely to be X-ray binaries with masses of at least $3 - 20 M_\odot$ (implied by their Eddington luminosities) suggesting that they are possible blackhole candidates.

Summarizing, the main observational result reported in this Letter is the unambiguous detection in NGC 253 of a hot luminous component whose nature is, however, still to be clarified.

Acknowledgements. We thank R. Della Ceca and S. Molendi for helpful discussion. We also thank the SAX Team for contributing to the operations of the satellite and for continuous maintenance of the software. This research has made use of SAXDAS linearized and cleaned event files produced at the BeppoSAX Science Data Center. The referee, Andy Ptak, has helped, with his comments and remarks, to improve the paper. We acknowledge partial financial support from the Italian Space Agency (ASI) and MURST.

3. References

- Bhattacharya, D., et al. 1994, *ApJ*, 437, 173
- Bookbinder, J., et al. 1980, *ApJ* 237, 647
- Bradamante, F., Matteucci, F., & D'Ercole, A. 1998, *A&A*, in press
- Cappi, M., et al. 1998, to appear in *Adv. Space Res.* proceedings of 32nd Scientific Assembly of Cospar

- Dahlem, M., Heckman, T., & Fabbiano, G. 1995, ApJ, 442, L49
- Dahlem, M., Weaver, K.A., & Heckman, T.M. 1998, ApJS, in press
- Dickey, J.M. & Lockman, F.J., 1990, ARA&A, 28, 215
- Fabbiano, G., 1988, ApJ, 330, 672
- Heckman, T.M., Armus, L., & Miley, G.K. 1990, ApJS, 74, 833
- Hogg, D.W., et al. 1998 press (astro-ph/9804129)
- Kaneda, H., et al. 1997, ApJ, 491, 638
- Madau, P., et al. 1996, MNRAS, 283, 1388
- Makishima, K. 1994, in New Horizon of X-Ray Astronomy, ed. F.Makino & T.Ohashi (Tokyo: Universal Academy Press), 171
- Makishima, K. 1995, in Elementary Processes in Dense Plasmas, ed. S.Ichimarui & S.Ogata (Reading: Addison-Wesley), 47
- Nakai, N., et al. 1987, PASJ, 39, 685
- Ohashi, T., et al. 1990, ApJ, 365, 180
- Paglione, T., Tosaki, T., & Jackson, J. 1996, ApJ, 454, L117
- Ptak, A., et al. 1997, AJ, 113, 1286
- Read, A.M., Ponman, T.J., & Strickland, D.K. 1997, MNRAS, 286, 626
- Rephaeli, Y., Gruber, D., & Persic, M., 1995, A&A, 300, 91
- Rieke, G.H. et al. 1980, ApJ, 238, 24
- Serlemitsos, P., Ptak, A., & Yaqoob, T. 1996, in "The Physics of Liners", ed. M.Crableous et al., 70
- Suchkov, A.A., et al. 1994, ApJ, 430, 511
- Telesco, C. 1988, ARA&A, 26, 343
- Valinia, A., & Marshall, F.E. 1998, ApJ, in press (astro-ph/9804012)
- Yaqoob, T., et al. 1995, ApJ, 455, 508

Table 3: Two component-thermal models.

Model	kT_{soft} keV	Ab_{soft} α -el. Fe, Ni	N_H^{hard} $\times 10^{22} \text{ cm}^{-2}$	kT_{hard} keV	Ab_{hard} α -el. Fe, Ni	χ^2/dof
RS	$0.88^{+0.22}_{-0.05}$	$1.52^{+0.20}_{-0.72}$	$1.28^{+0.26}_{-0.20}$	$5.62^{+0.41}_{-0.20}$	≤ 0.80	246.6/237
		$0.19^{+0.03}_{-0.05}$			$0.25^{+0.05}_{-0.06}$	
Mekal	$0.88^{+0.13}_{-0.13}$	$1.69^{+0.02}_{-0.72}$	$1.30^{+0.63}_{-0.45}$	$5.60^{+0.70}_{-0.60}$	≤ 1.76	243.6/237
		$0.18^{+0.29}_{-0.07}$			$0.27^{+0.10}_{-0.08}$	

Notes: The value of the relative normalizations A_{LECS}/A_{MECS} is $\simeq 0.66 \pm 0.03$. Intervals are at 90% confidence for one interesting parameter.